Mineralogy and Petrology of Comet 81P/Wild 2 Nucleus Samples

Michael E. Zolensky, *et al.*

Science **314**, 1735 (2006);
DOI: 10.1126/science.1135842

Science (print ISSN 0036-8075; online ISSN 1095-9203) is published weekly, except the last week in December, by the American Association for the Advancement of Science, 1200 New York Avenue NW, Washington, DC 20005.

References and Notes

1. P. Tsou *et al.*, *J. Geophys. Res.* **109**, E12S01 (2004).
2. A. J. Westphal *et al.*, *Meteorit. Planet. Sci.* **39**, 1375 (2004).
3. G. J. Flynn, F. Hörz, S. Bajt, S. R. Sutton, *Lunar Planet. Sci.* **XXVII**, 369 (1996).
4. See the supporting material on *Science* Online.
5. K. Lodders, *Astrophys. J.* **591**, 1220 (2003).
6. E. Anders, N. Grevese, *Geochim. Cosmochim. Acta* **53**, 197 (1989).
7. M. E. Zolensky *et al.*, *Science* **314**, 1735 (2006).
8. S. A. Sandford *et al.*, *Science* **314**, 1720 (2006).
9. A. T. Kearsley *et al.*, *Meteorit. Planet. Sci.*, in press.
10. A. T. Kearsley, M. J. Burchell, F. Hörz, M. J. Cole, C. S. Schwandt, *Meteorit. Planet. Sci.* **41**, 167 (2006).
11. F. Hörz *et al.*, *Science* **314**, 1716 (2006).
12. D. E. Brownlee, in *Properties and Interactions of Interplanetary Dust*, Proceedings of the Eighty-fifth Colloquium, Marseille, France, 9–12 July 1984 (Reidel, Dordrecht, Netherlands, 1985), pp. 143–147.
13. G. J. Flynn, S. R. Sutton, in *Proceedings of the 20th Lunar and Planetary Science Conference* (Lunar and Planetary Institute, Houston, TX, 1990), pp. 335–342.
14. J. Kissel, in *Advances in Mass Spectroscopy 1985, Proceedings of the 10th International Mass Spectrometry Conference*, Swansea, UK, 9–13 September 1985 (Wiley and Sons, Hoboken, NJ, 1986), pp. 175–184.
15. E. K. Jessberger, *Space Sci. Rev.* **90**, 91 (1999).
16. L. S. Schramm, D. E. Brownlee, M. M. Wheelock, *Meteoritics* **24**, 99 (1989).
17. G. J. Flynn *et al.*, in *Physics, Chemistry, and Dynamics of Interplanetary Dust*, B. Å. S. Gustafson, M. S. Hanner, Eds. (Astronomical Society of the Pacific, San Francisco, 1996), pp. 291–294.
18. D. E. Brownlee *et al.*, *Lunar Planet. Sci.* **XXIV**, 205 (1993).

19. Four synchrotrons used in this effort are national user facilities supported in part by the U.S. Department of Energy, Office of Science, Office of Basic Energy Sciences, under contract numbers (with managing institutions in parentheses) DE-AC02-05CH11231 (Advanced Light Source, University of California), DE-AC02-06CH11357 (Advanced Photon Source, University of Chicago Argonne, LLC), DE-AC02-98CH10886 (National Synchrotron Light Source, Brookhaven Science Associates), and DE-AC03-765F00515 (Stanford Synchrotron Radiation Laboratory, Stanford University). Experiments were performed at the BL47XU in the SPring-8 with the approval of the Japan Synchrotron Radiation Research Institute. The European Synchrotron Radiation Facility provided synchrotron radiation facilities. Stardust was the fourth flight project of NASA's Discovery Program.

Supporting Online Material

www.sciencemag.org/cgi/content/full/314/5806/1731/DC1
SOM Text
Figs. S1 to S11
Tables S1 to S4
References

10 October 2006; accepted 20 November 2006
10.1126/science.1136141

REPORT

Mineralogy and Petrology of Comet 81P/Wild 2 Nucleus Samples

Michael E. Zolensky,[1]* Thomas J. Zega,[2] Hajime Yano,[3] Sue Wirick,[4] Andrew J. Westphal,[5] Mike K. Weisberg,[6] Iris Weber,[7] Jack L. Warren,[8] Michael A. Velbel,[9] Akira Tsuchiyama,[10] Peter Tsou,[11] Alice Toppani,[12,13] Naotaka Tomioka,[14] Kazushige Tomeoka,[14] Nick Teslich,[12] Mitra Taheri,[2] Jean Susini,[15] Rhonda Stroud,[2] Thomas Stephan,[7] Frank J. Stadermann,[16] Christopher J. Snead,[5] Steven B. Simon,[17] Alexandre Simionovici,[18] Thomas H. See,[19] François Robert,[20] Frans J. M. Rietmeijer,[21] William Rao,[22] Murielle C. Perronnet,[1] Dimitri A. Papanastassiou,[23] Kyoko Okudaira,[3] Kazumasa Ohsumi,[24] Ichiro Ohnishi,[14] Keiko Nakamura-Messenger,[8] Tomoki Nakamura,[25] Smail Mostefaoui,[20] Takashi Mikouchi,[26] Anders Meibom,[20] Graciela Matrajt,[27] Matthew A. Marcus,[28] Hugues Leroux,[29] Laurence Lemelle,[18] Loan Le,[8] Antonio Lanzirotti,[30] Falko Langenhorst,[31] Alexander N. Krot,[32] Lindsay P. Keller,[1] Anton T. Kearsley,[33] David Joswiak,[27] Damien Jacob,[29] Hope Ishii,[12] Ralph Harvey,[34] Kenji Hagiya,[35] Lawrence Grossman,[17,36] Jeffrey N. Grossman,[37] Giles A. Graham,[12] Matthieu Gounelle,[20,33] Philippe Gillet,[18] Matthew J. Genge,[38] George Flynn,[39] Tristan Ferroir,[18] Stewart Fallon,[12] Denton S. Ebel,[40] Zu Rong Dai,[12] Patrick Cordier,[29] Benton Clark,[41] Miaofang Chi,[12] Anna L. Butterworth,[5] Donald E. Brownlee,[27] John C. Bridges,[42] Sean Brennan,[43] Adrian Brearley,[21] John P. Bradley,[12] Pierre Bleuet,[15] Phil A. Bland,[33,38] Ron Bastien[8]

The bulk of the comet 81P/Wild 2 (hereafter Wild 2) samples returned to Earth by the Stardust spacecraft appear to be weakly constructed mixtures of nanometer-scale grains, with occasional much larger (over 1 micrometer) ferromagnesian silicates, Fe-Ni sulfides, Fe-Ni metal, and accessory phases. The very wide range of olivine and low-Ca pyroxene compositions in comet Wild 2 requires a wide range of formation conditions, probably reflecting very different formation locations in the protoplanetary disk. The restricted compositional ranges of Fe-Ni sulfides, the wide range for silicates, and the absence of hydrous phases indicate that comet Wild 2 experienced little or no aqueous alteration. Less abundant Wild 2 materials include a refractory particle, whose presence appears to require radial transport in the early protoplanetary disk.

The nature of cometary solids is of fundamental importance to our understanding of the early solar nebula and protoplanetary history. Until now, we have had to study comets from afar using spectroscopy or settle for analyses of interplanetary dust particles (IDPs) of uncertain provenance. We report here mineralogical and petrographic analyses of particles derived directly from comet 81P/Wild 2.

All of the Wild 2 particles we have thus far examined have been modified in various ways by the capture process, in which cometary particles punched into the silica aerogel capture media, making various types of tracks and disaggregating into grains distributed along the tracks. All particles that may have been loose aggregates ("traveling sand piles") disaggregated into individual components, with the larger, denser components penetrating more deeply into the aerogel, making thin tracks with terminal grains (fig. S1). Individual grains experienced heating effects that produced results ranging from excellent grain preservation to melting (Fig. 1); such behavior was expected (*1*–*3*). What is remarkable is the extreme variability of these modifications and the fact that unmodified and severely modified materials can be found within 1 μm of each other, requiring tremendous local temperature gradients. Fortunately, we have an internal gauge of impact collection heating. Fe-Ni sulfides are ubiquitous in the Wild 2 samples and are very sensitive indicators of heating, and accurate chemical analyses can reveal which have lost S and which have not (and are therefore stoichiometric) (Fig. 2). Our surveys show that crystalline grains are found along the entire lengths of tracks, not just at track termini (fig. S1).

There appears to be very limited contamination from the spacecraft in the aerogel. Potential problems with secondary impacts (cometary grains striking the spacecraft, ricocheting, and splashing onto the aerogel) failed to materialize (*4*).

We have harvested samples from 52 tracks and have obtained a substantial understanding of the mineralogy of 26 of these. These tracks were chosen at random from those of average length. Analyses have also been performed on impact residues in seven aluminum foil craters >50 μm in diameter and on over 200 craters <5 μm in diameter (*5*). Crystalline materials are abundant in comet Wild 2 and many are coarse-grained relative to the submicrometer scales characteristic of many anhydrous IDPs and interstellar dust populations (*6*). Of the best-studied 26 tracks, 8 are dominated by olivine [$(Mg,Fe)_2SiO_4$] grains (tracks 1, 22, 26, 43, 57, 68, 71, and 77); 7 by low-Ca pyroxene [$(Mg,Fe)SiO_3$] (tracks 17, 20, 24, 27, 32, 41, and 69); 3 by a fairly equal amount of olivine and pyroxene (tracks 5, 10, and 35); and the remaining 8 by other minerals, mainly Fe-Ni sulfides. One of the latter tracks contains predominantly refractory minerals, one contains Na-silicate minerals, and five (tracks 36, 38, 42, 52, and 59) are dominated by ~5-μm-sized sulfide grains. These results suggest that crystalline materials are abundant in Wild 2.

In the seven large craters in aluminum foil that we examined, one contains only remnants of stoichiometric olivine, three are dominated by Mg-

silicates and sulfide, and two contain a mixture of mafic silicates and Na- and Ca-rich silicates. The last complex impact feature has overlapped bowl-shaped depressions containing residues with a heterogeneous collection of stoichiometric compositions, suggesting impact by an aggregate of micrometer-scale grains of Ca-rich clinopyroxene, Mg-rich pyroxene (probably enstatite), and a mixture of Fe-Ni sulfides, as well as grains composed of finely mixed silicate and sulfide. Just over half of the residue-bearing very small craters we examined contain mixtures of silicate and sulfur-bearing residue, whereas the others are mainly monomineralic olivine, pyroxene, and Fe-Ni sulfides, with occasional preservation of crystalline material.

Olivine, one of the most abundant minerals in the solar system (*7*–*9*), is present in the majority of Wild 2 particles. Its observed grain sizes range from submicrometer to over 10 μm. Wild 2 olivine has an extremely wide compositional range, from Fo_4 to Fo_{100} ["Fo" being the 100 × molar Mg/(Mg+Fe) ratio for olivine, just as "En" is the same ratio for low-Ca pyroxenes] (Fig. 3), with a pronounced frequency peak at Fo_{99}. Although it is possible that collection effects have biased surviving olivines to the most refractory, Mg-rich compositions, the abundance of Fe-rich olivine among the Wild 2 samples suggests that this effect has been minor. One olivine crystal in track 22 was found to display dramatic reverse chemical zoning, from the Fo_{70} core to the Fo_{92} rim. It is clear that these grains were not equilibrated during capture, because we would then observe a greatly reduced compositional range and a peak at a high Fe (low Fo value) concentration (*1*, *2*, *10*, *11*).

Wild 2 olivines include varieties with very elevated MnO, Al_2O_3, and Cr_2O_3 contents, up to 6.45, 0.71, and 1.46 weight %, respectively. About 25% of these Mn- and Cr-rich olivines contain <<1% FeO. Olivines with enrichments in these elements have been reported in carbonaceous chondrites, micrometeorites, and chondritic IDPs, though they are very rare (*12*–*16*). The compositions of the Mn- and Cr-rich olivines in the Wild 2 samples are similar to those in IDPs, carbonaceous chondrites, and unequilibrated ordinary chondrites (fig. S2). Many Wild 2 olivines contain inclusions of other phases, notably Fe-Cr-Ti oxides (including chromite), but thus far, melt inclusions have not been observed within any silicates. Olivine with low Fe and elevated Mn has been proposed to form from condensation in the protosolar nebula (*12*).

Wild 2 olivine-dominated grains are commonly polycrystalline, with some interstitial glass, which could be indigenous cometary glass. One fragment from the wall of the 1-cm-long track 35 was investigated by microtomography (*17*) and found to have a microporphyritic texture with olivine crystals (~Fo_{80}) set within lower-density fine-grained material, probably glass. From the manner in which the enclosing aerogel wraps around this particular grain without intruding into it, the glass appears to be indigenous. This fragment has an obvious igneous origin and resembles a microporphyritic chondrule. A terminal grain from track 26 consists of an intergrowth of fayalite (Fo_4) and tridymite, another texture observed in some chondrules.

Both low- and high-Ca pyroxenes are present among the Wild 2 grains, with the former being dominant. In some cases, synchrotron x-ray diffraction (SXRD) or selected-area electron diffraction

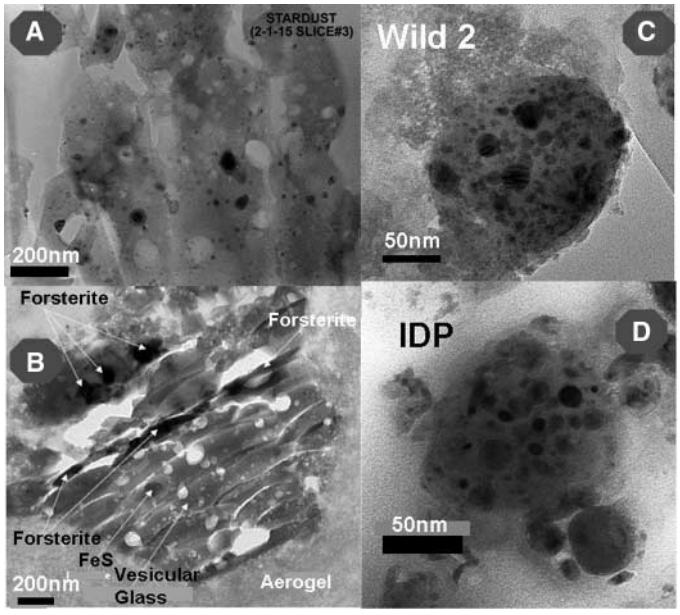

Fig. 1. Bright-field TEM images of Wild 2 grains. (**A**) View of the compressed and vesicular melted aerogel surrounding grains and lining track walls. Dark gray and black objects are admixed silicates, Fe-Ni metal, and Fe-Ni sulfides. (**B**) Captured Wild 2 grain composed predominantly of forsterite and Fe-sulfides, mantled by compressed-to-melted aerogel. (**C**) Glassy body from Wild 2 track 10, resembling a GEM; rounded dark inclusions are predominantly Fe-Ni metal, Fe-Ni sulfides, and ferromagnesian silicates. (**D**) GEM from an anhydrous chondritic IDP; rounded dark inclusions are predominantly Fe-Ni metal, Fe-Ni sulfides, and ferromagnesian silicates.

[1]Astromaterials Research and Exploration Science, NASA Johnson Space Center, Houston, TX 77058, USA. [2]Naval Research Laboratory, Code 6360, 4555 Overlook Avenue SW, Washington, DC 20375, USA. [3]JAXA-ISAS, 3-1-1 Yoshinodai, Sagamihara, Kanagawa 229-8510, Japan. [4]National Synchrotron Light Source, Brookhaven National Laboratory, Upton, NY 11973, USA. [5]Space Sciences Laboratory, University of California, 7 Gauss Way, Berkeley, CA 94720–7450, USA. [6]Department of Physical Sciences, Kingsborough Community College (CUNY), Brooklyn, NY 11235, USA. [7]Institut für Planetologie, Westfälische Wilhelms-Universität Münster, Wilhelm-Klemm-Strasse 10, 48149 Münster, Germany. [8]Jacobs Sverdrup, Engineering Science Contract Group, Houston, TX 77058, USA. [9]Department of Geological Sciences, 206 Natural Science Building, Michigan State University, East Lansing, MI 48824–1115, USA. [10]Department of Earth and Space Science, Osaka University, 1-1 Machikaneyama-cho, Toyonaka 560-0043, Japan. [11]Jet Propulsion Laboratory, M/S 183-501, 4800 Oak Grove Drive, Pasadena, CA 91109, USA. [12]Institute for Geophysics and Planetary Physics, Lawrence Livermore National Laboratory, Livermore, CA 94550, USA. [13]Centre de Spectrometrie Nucleaire et de Spectrometrie de Masse, Bâtiment 104, 91405 Orsay Campus, France. [14]Department of Earth and Planetary Sciences, Faculty of Science, Kobe University, Nada, Kobe 657-8501, Japan. [15]European Synchrotron Radiation Facility, Boîte Postale 220, 38043 Grenoble, France. [16]Department of Physics, Washington University, St. Louis, MO 63130, USA. [17]Department of Geophysical Sciences, The University of Chicago, 5734 South Ellis Avenue, Chicago, IL 60637, USA. [18]Laboratoire de Sciences de la Terre, Ecole Normale Superieure de Lyon, 46, Allee d'Italie, 69007 Lyon, France. [19]Engineering Science Contract/Barrios Technology, ARES/JSC, Houston, TX 77258–8447, USA. [20]Museum National d'Histoire Naturelle, Laboratoire d'Etude de la Matiere Extraterrestre, USM 0205 (LEME), Case Postale 52, 57 Rue Cuvier, 75005 Paris, France. [21]Department of Earth and Planetary Sciences, University of New Mexico, MSC 03-2040, Albuquerque, NM 87131–0001, USA. [22]Savannah River Ecology Lab, Aiken, SC 29801, USA. [23]Science Division, Jet Propulsion Laboratory, M/S 183-335, 4800 Oak Grove Drive, Pasadena, CA 91109, USA. [24]Institute of Materials Structure Science, Tsukuba-shi, Ibaraki-ken 305, Japan. [25]Department of Earth and Planetary Sciences, Faculty of Sciences, Kyushu University, Hakozaki, Fukuoka 812-8581, Japan. [26]Department of Earth and Planetary Science, University of Tokyo, Hongo, Bunkyo-ku, Tokyo 113-0033, Japan. [27]Department of Astronomy, University of Washington, Seattle, WA 98195, USA. [28]Advanced Light Source, Lawrence Berkeley National Laboratory, 1 Cyclotron Road, MS 2R2100, Berkeley, CA 94720, USA. [29]Laboratoire de Structure et Propriétés de l'Etat Solide, Bâtiment C6, Université des Sciences et Technologies de Lille, 59655 Villeneuve d'Ascq, France. [30]Consortium for Advanced Radiation Sources, The University of Chicago, Chicago, IL 60637, USA. [31]Institute of Geosciences, Friedrich-Schiller-University Jena, Burgweg 11, D-07749 Jena, Germany. [32]Hawaii Institute of Geophysics and Planetology, University of Hawaii, Honolulu, HI 96822, USA. [33]Impact and Astromaterials Research Centre, Department of Mineralogy, Natural History Museum, Cromwell Road, London, SW7 5BD, UK. [34]Department of Geology, Case Western Reserve University, Cleveland, OH 44106, USA. [35]Graduate School of Life Science, University of Hyogo, Koto 3-2-1, Kamigori, Ako-gun, Hyogo 678-1297, Japan. [36]Enrico Fermi Institute, The University of Chicago, 5640 South Ellis Avenue, Chicago, IL 60637, USA. [37]U.S. Geological Survey, 954 National Center, Reston, VA 20192, USA. [38]Impact and Astromaterials Research Centre, Department of Earth Sciences and Engineering, Imperial College of Science Technology and Medicine, Prince Consort Road, London, SW7 2AZ, UK. [39]Department of Physics, State University of New York, Plattsburgh, NY 12901, USA. [40]Department of Earth and Planetary Sciences, American Museum of Natural History, Central Park West at 79th Street, New York, NY 10024, USA. [41]Lockheed Martin Astronautics, Denver, CO 80201, USA. [42]Planetary and Space Sciences Research Institute, Open University, Milton Keynes, MK7 6AA, UK. [43]Stanford Linear Accelerator Center, Menlo Park, CA 94025, USA.

*To whom correspondence should be addressed. E-mail: michael.e.zolensky@nasa.gov

(SAED) patterns reveal low-Ca pyroxenes to be orthoenstatite, requiring slow cooling (*18*), but in the majority of cases we have only energy-dispersive x-ray analyses and are not certain whether we have ortho- or clinopyroxene. The compositional range displayed by the low-Ca pyroxene is also very extensive, from En_{52} to En_{100}, with a significant frequency peak centered at En_{95} (Fig. 3). Low-Ca pyroxene usually coexists with olivine, but the Mg/Fe ratios for coexisting phases are not always similar. Track 17 contains olivine in the range $Fo_{55–69}$, whereas associated low-Ca pyroxene is $En_{52–96}$. Flash heating during sample collection may account for this disparity, because olivine equilibrates faster than orthopyroxene under identical circumstances (*19*). Diopside occurs in several grains, usually in association with low-Ca pyroxene. A Ti-, Al-rich diopside is abundant within the calcium-, aluminum-rich inclusion (CAI)–like particle.

Sulfides are the only mineral group found in all extraterrestrial materials. Fe-Ni sulfides are also ubiquitous in the Wild 2 grains, grading from sulfides apparently melted and mixed with Fe-Ni metal, all the way to apparently unmodified FeS and pentlandite [$(Fe,Ni)_9S_8$] grains (fig. S3). Several tracks (such as track 59) have FeS- or pentlandite-dominated terminal grains. In this paper, we collectively refer to troilite (stoichiometric FeS) and pyrrhotite ($Fe_{1-x}S$) as FeS because the exact stoichiometry and structure are unknown in most instances. A plot of analyses of Wild 2 Fe-Ni sulfides (Fig. 2) shows that many have compositions close to that of FeS, with less than 2 atom % Ni. Only two pentlandite grains have been found. The complete lack of compositions in between these (intermediate solid solution compositions) suggests (but does not require) that FeS and pentlandite condensed as crystalline species [that is, did not condense as amorphous phases, which later became annealed (*20*)]. The remaining Fe-Ni sulfides (approximately half) have compositions that reflect progressive loss of S, because they trend from FeS directly toward the Fe apex. SAED patterns of these S-depleted phases show the presence of two different lattices: strong maxima for a Fe-Ni sulfide phase and a much finer pattern consistent with a metal phase, but which could be an oxide. Loss of S from Fe-Ni sulfides is almost certainly a result of capture heating and could be used to gauge the degree of capture modification of the enclosing Wild 2 grains. The two verified pentlandite crystals in only two Wild 2 tracks are intriguing because this phase is frequently an indicator of low-temperature metamorphism under oxidizing conditions and/or of aqueous alteration (*21*).

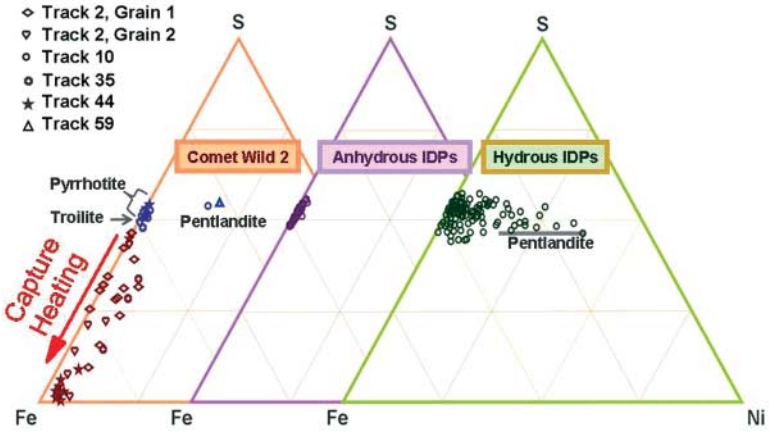

Fig. 2. Composition ranges of Fe-Ni sulfides from six grains from five Wild 2 particle tracks. Grains from track walls as well as track termini were analyzed. Most Wild 2 sulfides are probably a mixture of troilite and pyrrhotite, and two grains of pentlandite are present. Many sulfides plot with non-stoichiometric, low-S compositions reflecting capture heating. The corresponding composition ranges for hydrous and anhydrous chondritic IDPs (*21*) are also shown. Anhydrous chondritic IDPs contain only troilite and pyrrhotite, whereas the hydrous chondritic IDPs also have equally abundant Ni-rich sulfides, including pentlandite. With the exception of the two identified pentlandite crystals, the Wild 2 grains have the same Fe-Ni sulfide composition range as the anhydrous chondritic IDPs.

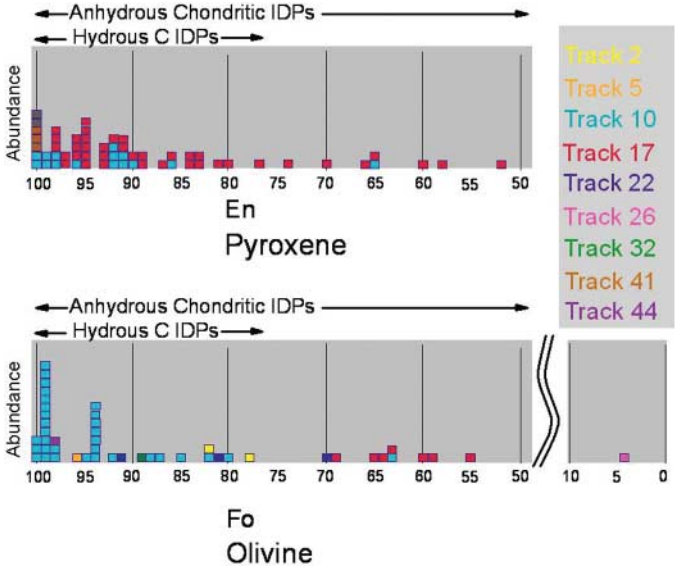

Fig. 3. Composition ranges of low-Ca pyroxene (En) and olivine (Fo) in grains from nine Wild 2 particles (tracks). Grains from track walls as well as track termini were analyzed, but predominantly the latter. The corresponding composition ranges for hydrous and anhydrous chondritic IDPs are also shown (*34*). The Wild 2 grains have the same olivine and low-Ca pyroxene composition ranges as the anhydrous chondritic IDPs, although the presence of mixed hydrous and anhydrous materials is compatible with these data.

A Cu-Fe sulfide, probably cubanite ($CuFe_2S_3$), is present within terminal grains in at least two tracks (tracks 22 and 26). Cubanite is occasionally encountered in extraterrestrial materials, most commonly in carbonaceous chondrites. (Fe,Zn)S was found within a terminal grain from track 22. If it can be established that this phase is in equilibrium with FeS and metal, it may be appropriate to apply the sphalerite cosmobarometer to this particular particle (*22*).

Fe-Ni metal is present as nanoscale beads in significant quantities in most tracks, partly as a product of capture heating of Fe-Ni sulfides, but the high abundance of Ni in these shows that some of this metal is intrinsic to the comet particles. In addition, tracks 38 and 43 have ~5-μm-sized Fe-Ni metal terminal grains (Ni/Fe ~ 0.03), which appear to be indigenous cometary phases.

Some Wild 2 grains contain alkali-rich mineral assemblages, including phases in tracks 3 and 16 with compositions corresponding to K-feldspar (SAED patterns suggest a feldspar-like structure, but the exact phase is not known) and what appears to be eifelite [$KNa_2(MgNa)Mg_3Si_{12}O_{30}$] (track 56). Eifelite is in the osumilite mineral group, whose members have been reported in iron meteorites, as well as enstatite and ordinary chondrites (*23*), where they formed from a combination of igneous and metasomatic processes. In addition, alkali-rich silicate material is present in some of the larger craters in aluminum foil, but it has not been well characterized.

Transmission electron microscope (TEM) observations of some tracks revealed the presence of carbonaceous phases. In the terminal grain from tracks 10, 13, 27, 41, 57, and 58, there are submicrometer-sized subgrains of poorly crystalline carbon. Some of these are attached to Fe-Ni sulfides, suggesting a genetic relationship.

No evidence of phyllosilicates or indigenous carbonate has been seen in any Wild 2 samples. Despite the fact that substantial heating and structural modification accompanied the collection of many grains in the aerogel, we would have seen characteristic compositions, grain morphologies, and lattice fringes of phyllosilicates or carbonates had they

been present (*2*, *3*, *24*). Serpentine and Ca carbonates of the same sizes as in IDPs have been successfully captured in silica aerogel even at velocities 1 km/s higher than those experienced at Wild 2, in both laboratory simulations and actual IDP collection in Earth orbit aboard the Mir space station. In instances where phyllosilicates have been dehydrated, rendered amorphous, or recrystallized during capture in silica aerogel, characteristic grain morphologies and basal lattice spacings are formed, which signal the original mineralogy (*2*, *24*). Thus, the lack of these phases among the ~50 Wild 2 grains we have so far well characterized suggests that they could not have composed more than a few percent of the more coarse-grained fraction of captured Wild 2 samples.

Along most tracks are found abundant rounded, glassy silicate bodies containing submicrometer-sized beads of silicates, Fe-Ni sulfides, and Fe-Ni metal (Fig. 1, C and D). In some respects these bodies are similar to the bits of glass with embedded metal and sulfides (GEMS) common to most anhydrous chondritic IDPs (*6*), as well as one peculiar clast in the unequilibrated carbonaceous chondrite Ningqiang (*25*). It has been proposed that GEMS are among the most primitive of solar system materials, possibly recording the radiation environment of the early Sun or of a presolar environment (*6*).

The GEMS-like bodies in the tracks often stand out texturally from the typical and dominating aerogel capture medium in terms of composition, structure, and morphology. A composition comparison with true GEMS (Table 1) shows similarities but also important differences. For example, compared to the GEMS, the glassy bodies in the tracks have low Fe as compared to Mg and S (Table 1). Additionally, there exists a textural difference between GEMS and the Stardust glassy bodies. In GEMS, the inclusions are scattered about randomly and grade from nanometer- to submicrometer-sized objects (*6*). The glassy bodies in the aerogel tracks have coarser-grained inclusions and a tendency for these to be arranged in nonrandom patterns. Also, there are sometimes no distinct boundaries between the GEMS-like objects and the embedding aerogel. In addition, some of the metal grains in the Stardust glassy bodies have S-rich rims, which are not observed in GEMS. Because <5% of GEMS have isotopic compositions very different from terrestrial values (*26*), we have not been able to determine which, if any, of the glass bodies in the aerogel collectors are cometary "GEMS" and which might be formed as a result of the melting and intermingling of fine-grained cometary matter with aerogel during the capture process.

Table 1. Quantitative energy-dispersive x-ray spectral analyses (atomic %) of two GEMS-like objects embedded in the aerogel of track 35 (GEMS 1 and 2) compared with actual GEMS in a chondritic IDP and CI chondrite (CI) abundances.

Element (atom %)	GEMS-like 1 (60 nm in diameter)	GEMS-like 2 (100 nm in diameter)		GEMs in IDPs (*6*)			CI (*39*, *40*)
O	64.95	65.8	65.7	75.3	61.9	56.2	49.7
Mg	6.3	3.5	4.6	1.2	2.9	22.3	10.3
Si	26.4	28.4	26.0	19.1	16.9	13.3	11.5
S	1.75	1.65	2.7	1.2	6.1	3.2	5.7
Ca	0.1	0.1	0.15	Nd	0.15	nd	0.3
Cr	trace	trace	trace	0.2	0.3	0.1	0.3
Mn	0.1	0.1	0.15	0.1	nd	nd	0.2
Fe	0.3	0.2	0.5	2.2	11.1	4.2	20.0
Ni	0.1	0.1	0.2	0.4	nd	0.1	1.1
Al	nd	nd	nd	0.5	0.8	0.6	0.9

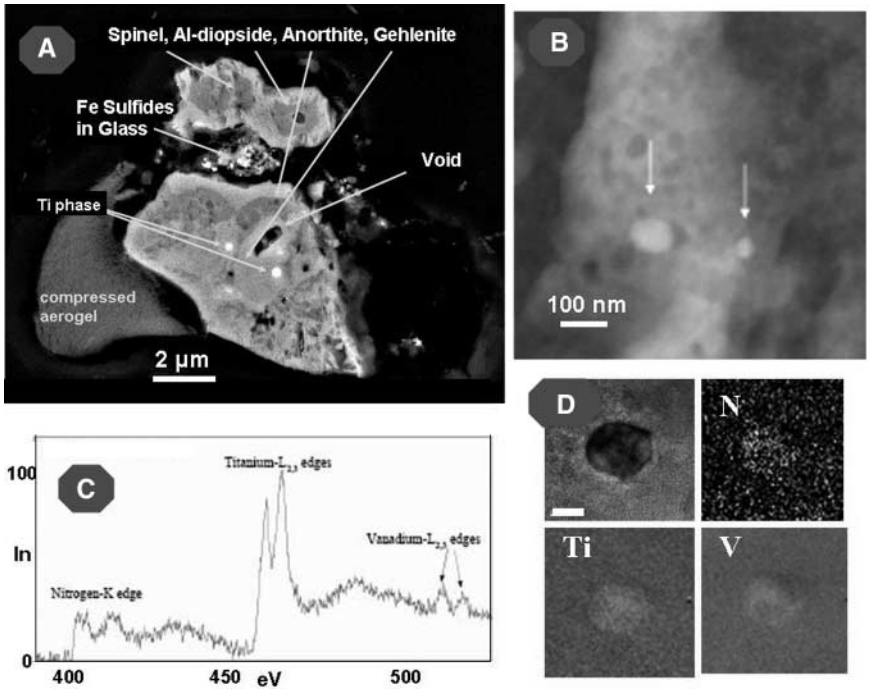

Fig. 4. The CAI-like grain from track 25. (**A**) Backscattered electron (BSE) image of the CAI-like grain from track 25, showing the gray shell of compressed-to-melted aerogel at lower left. (**B**) High-angle annular dark-field TEM image of two osbornite grains (arrows) within spinel. (**C**) EELS spectrum of an osbornite grain showing peaks for N, Ti, and V; scales represent intensity (In) and energy (in electron volts). (**D**) EELS element maps of an orbornite grain: BSE, N, Ti, and V. Scale bar, 40 nm.

One Wild 2 sample (track 25) has received special attention (Fig. 4) because it consists of very refractory minerals, including anorthite; a Ca-, Al-, Ti-rich clinopyroxene; gehlenite; spinel; corundum; FeS; V-bearing osbornite [(Ti,V)N]; and a phase that is probably perovskite. The osbornite occurs as sub–100-nm-sized grains within spinel, and its identification was carefully established by a combination of electron energy-loss spectroscopy (EELS) and SAED work; it may be associated with titanium oxide. The largest terminal grain from track 25 is ^{16}O-rich (*27*).

Track 25 yielded a terminal particle and at least four major subparticles, which have been characterized. These particles exhibit some similarities to and differences from the CAIs found in carbonaceous chondrites; in particular, they have mineralogies similar to CAIs in CV3 and CM2 chondrites (*5*) (CV3 and CM2 are among the most abundant types of carbonaceous chondrites), an important finding because the inclusions are known to be among the most primitive solar system objects (based on their mineralogy, reduced oxidation state, enrichments in refractory trace elements, isotopes, etc.).

The minerals within the Wild 2 CAI-like particle, especially the osbornite, require rather high temperatures for formation, possibly higher than 2000 K, depending on oxygen fugacity (*28*). According to equilibrium thermodynamic calculations, osbornite + spinel + Ca-rich clinopyroxene is a stable condensate assemblage in systems that are otherwise solar in composition only if their atomic C/O ratio lies between ~0.79 and ~0.97, which is well above the solar value of 0.5. The presence of a CAI-like particle in comet Wild 2 appears to require large-scale radial transport in the protoplanetary disk (*29*, *30*). Although the anorthite in this particle is too small for a meaningful search for evidence of ^{26}Al, this may prove possible in some refractory Wild 2 grains.

The recovered Wild 2 samples are mixtures of crystalline and amorphous materials. Analytical

electron microscopy (AEM) analysis of grains from the upper, often bulb-shaped, portions of tracks shows that they typically have widely varying compositions, sometimes similar to chondrites for most elements except Si, even in severely heated and melted regions (Table 1) (*31*). The crystalline grains observed among the upper portions of individual tracks are almost always submicrometer in grain size. These observations suggest that the materials captured in the upper portions of the tracks are, in general, much finer-grained than the material at the end of the slender, so-called stylus tracks that almost always project from the bulb-like upper tracks (fig. S1). AEM of very small craters on the aluminum foil also reveals crystalline olivine, pyroxene, and sulfides derived from separate submicrometer components within micrometer-sized particles. Synchrotron x-ray fluorescence (SXRF) analyses (*31*) suggest that 65 to 90% of the collected grains' mass is found in the upper portions of tracks, and only 10 to 35% is represented by the track termini grains. Our emerging model of the structure of the captured grains is that many were predominantly very fine-grained (submicrometer-sized) loosely bound aggregates with a bulk chondritic composition, most also containing much larger individual crystals (most commonly) of olivine, pyroxene, and Fe-Ni sulfides. Out of the ~70 tracks we have carefully photodocumented, only 2 appear to have no visible terminal grains, which indicates that practically all collected cometary particles contained some of these larger grains, which therefore probably served to nucleate the cometary particles. This view is supported by some of the larger crater morphologies observed on the Stardust Al foils, which have a multilobe appearance rather than being simple hemispherical craters (fig. S5) and can contain diverse subgrain compositions. This physical structure is consistent with several chondritic materials, most notably chondritic IDPs (*13*). In general, the captured Wild 2 grains are much finer-grained than the bulk of meteoritic matrix materials or IDPs.

Considering first the ferromagnesian mineral–dominated Wild 2 grains, the olivine and pyroxene crystals have the same range of Mg, Fe, Mn, and Cr compositions as those in anhydrous chondritic IDPs [with the exception of a single Fo_4 terminal grain (Fig. 3)] and are very similar to those in type 2 and some type 3 carbonaceous chondrites. The lack of hydrous phases among the Wild 2 samples precludes a common origin with type 1 or 2 chondrites. The type 3 carbonaceous chondrites (including primitive chondrites Acfer 094 and ALHA 77307) (*32*, *33*) and hydrous chondritic IDPs generally have narrower or somewhat equilibrated olivine and pyroxene compositional ranges (*34*). However, with the exception of the two pentlandite grains encountered in our examination, the Fe-Ni sulfide compositions of the Wild 2 grains are similar only to the anhydrous chondritic IDPs. Hydrous IDPs and all chondrites contain large amounts of pentlandite and low-Ni pentlandite (*21*). In addition, the absence of any identified aqueous alteration products in the Wild 2 grains (no phyllosilicates or indigenous carbonates, etc.) eliminates the hydrous chondritic materials from direct comparison.

No nuclear tracks (which are linear defects made by penetrating solar flare particles from the Sun) have yet been observed among Wild 2 samples. It is possible that the majority of these, if ever present, were annealed during capture, although some were observed in crater residue on the Long Duration Exposure Facility and in lunar silicate grains shot into aerogel (*35*).

In summary, the bulk of the Wild 2 samples appear to be weakly constructed mixtures of nanometer-scale grains with occasional much larger (>1 μm) ferromagnesian silicates, Fe-Ni sulfides, and Fe-Ni metal. The restricted compositional ranges of the sulfides and very wide range for silicates suggest that Wild 2 experienced little or no aqueous alteration. Of known extraterrestrial materials, the anhydrous chondritic IDPs and anhydrous micrometeorites are most similar to the Wild 2 grains, and in fact a cometary origin for anhydrous IDPs has been suspected for many years (*36*), whereas models of weakly constructed comet grains have been popular for years (*37*). The similarity of Wild 2 samples to some IDPs demands reexamination of the latter with new eyes, for there are some apparent differences. For example, Fe-Cr-Ti oxides have not been reported as inclusions in IDP olivines, nor has orthoenstatite been reported (*13*). The very wide ranges of olivine and low-Ca pyroxene compositions in Wild 2 require a wide range of formation conditions, including diverse temperatures and oxygen fugacities, probably reflecting different locations in the protoplanetary disk. It is critical to determine the role of annealing in cometary grain formation, but this cannot be done with the mineralogic data in hand.

The presence of a refractory particle resembling a meteoritic CAI among the Wild 2 grains raises many new questions. IDPs are believed to contain samples of both asteroids and comets, and wholly refractory IDPs were identified two decades ago (*31*, *32*) but have received very little attention. In mineralogical terms, the Wild 2 CAI-like particle appears similar to these poorly understood IDPs and is similar (though finer-grained) in various respects to CAI from CM, CR, and CH-CB carbonaceous chondrites. The presence of CAI-like material in a comet appears to require substantial radial transport of material across the early protoplanetary disk, as does the rather wide range of olivine and pyroxene compositions discussed above.

The lack of aqueous alteration products in Wild 2 samples is in clear contrast to the mineralogy reported for comet Tempel 1, based on Spitzer Space Observatory data in support of the Deep Impact mission (*9*). This mineralogical difference could be due to differences in the geological histories of Jupiter-family comets (*38*).

References and Notes

1. R. A. Barrett, M. E. Zolensky, R. Bernhard, *Lunar Planet. Sci.* **24**, 65 (1993).
2. F. Hörz, M. E. Zolensky, R. P. Bernhard, T. H. See, J. L. Warren, *Icarus* **147**, 559 (2000).
3. M. J. Burchell, G. Graham, A. Kearsley, *Annu. Rev. Earth Planet. Sci.* **34**, 385 (2006).
4. These issues are treated at greater length in the supporting material on *Science* Online.
5. F. Hörz *et al.*, *Science* **314**, 1716 (2006).
6. J. P. Bradley, *Science* **265**, 925 (1994).
7. E. K. Jessberger, A. Christoforidis, J. Kissel, *Nature* **332**, 691 (1988).
8. M. E. Lawler, D. E. Brownlee, S. Temple, M. M. Wheelock, *Icarus* **80**, 225 (1989).
9. C. Lisse *et al.*, *Science* **313**, 635 (2006).
10. J. Akai, *Proc. NIPR Symp. Antarct. Meteorites* **3**, 55 (1990).
11. M. E. Zolensky, W. H. Kinard, *Adv. Space Res.* **13**, 75 (1993).
12. W. Klöck, K. L. Thomas, D. S. McKay, H. Palme, *Nature* **339**, 126 (1989).
13. F. J. M. Rietmeijer, in *Planetary Materials*, J. J. Papike, Ed. (Mineralogical Society of America, Washington, DC, 1998), pp. 2-1–2-95.
14. M. Gounelle *et al.*, *Meteorit. Planet. Sci.* **37**, A55 (2002).
15. S. B. Simon, L. Grossman, *Meteorit. Planet. Sci.* **38**, 813 (2003).
16. M. K. Weisberg, H. C. Connolly, D. S. Ebel, *Meteorit. Planet. Sci.* **39**, 1741 (2004).
17. A. Tsuchiyama, *Lunar Planet. Sci. Conf.* **XXXVII**, abstract 2001 (2006).
18. W. A. Deer, R. A. Howie, J. Zussman, *Rock-Forming Minerals, Volume 2A, Single-Chain Silicates* (Longman, London, 1978).
19. J. Ganguly, V. Tazzoli, *Am. Mineral.* **79**, 930 (1994).
20. D. Vaughan, J. Craig, *Mineral Chemistry of Metal Sulfides* (Cambridge Univ. Press, Cambridge, 1978).
21. M. E. Zolensky, K. Thomas, *Geochim. Cosmochim. Acta* **59**, 4707 (1995).
22. M. N. Hutchison, S. D. Scott, *Geochim. Cosmochim. Acta* **47**, 101 (1983).
23. A. N. Krot, J. T. Wasson, *Meteoritics* **29**, 707 (1994).
24. R. A. Barrett, M. E. Zolensky, F. Hörz, D. J. Lindstrom, E. K. Gibson, *Proc. 19th Lunar Planet. Sci. Conf.* **22**, 203 (1992).
25. M. E. Zolensky *et al.*, *Meteorit. Planet. Sci.* **38**, 305 (2003).
26. S. Messenger, L. P. Keller, F. J. Stadermann, R. M. Walker, E. Zinner, *Science* **300**, 105 (2003).
27. K. D. McKeegan *et al.*, *Science* **314**, 1724 (2006).
28. D. Ebel, in *Meteorites and the Early Solar System II*, D. S. Lauretta, H. Y. McSween Jr., Eds. (Univ. of Arizona Press, Tucson, AZ, 2006), pp. 253–278.
29. F. Shu, H. Shang, A. E. Glassgold, T. Lee, *Science* **277**, 1475 (1997).
30. J. Cuzzi, S. Davis, A. Dobrovolskis, *Icarus* **166**, 385 (2003).
31. G. Flynn *et al.*, *Science* **314**, 1731 (2006).
32. A. J. Brearley, *Geochim. Cosmochim. Acta* **57**, 1521 (1993).
33. A. Greshake, *Geochim. Cosmochim. Acta* **61**, 437 (1997).
34. M. E. Zolensky, R. A. Barrett, *Meteoritics* **29**, 616 (1994).
35. P. Tsou *et al.*, *Lunar Planet. Sci. Conf.* **XXI**, 1264 (1990).
36. A. O. Nier, D. J. Shlutter, *Meteoritics* **28**, 675 (1993).
37. A. Li, M. Greenberg, *Astrophys. J.* **498**, L83 (1998).
38. D. E. Brownlee *et al.*, *Science* **314**, 1711 (2006).
39. E. Anders, M. Ebihara, *Geochim. Cosmochim. Acta* **46**, 2363 (1982).
40. In (*39*), carbon is ignored in the calculations and oxygen is calculated.

41. We thank the U.S. public for supporting the Stardust mission with valuable tax dollars and our many home institutions and funding agencies for making possible this concentrated 9-month-long analytical effort. The dedicated personnel of the Johnson Space Center Curation Facility were critical to our analytical efforts. We also thank our good friends at Lockheed Martin Space Systems for the wonderful spacecraft.

Supporting Online Material

www.sciencemag.org/cgi/content/full/314/5806/1735/DC1
Materials and Methods
Figs. S1 to S6
References

3 October 2006; accepted 20 November 2006
10.1126/science.1135842